

**Contains supplementary Materials and Methods, Supplementary table,
Supplementary Figures and legends**

Title: SLAMF1/CD150 regulates chemotaxis, autophagy and therapy responses in chronic lymphocytic leukemia patients

Authors: Cinzia Bologna^{1,2}, Roberta Buonincontri^{1,2}, Sara Serra², Tiziana Vaisitti^{1,2},
Valentina Audrito², Davide Brusa^{1,2}, Andrea Pagnani², Marta Coscia³, Giovanni D'Arena⁴,
Elisabetta Mereu⁶, Roberto Piva⁶, Richard R. Furman⁷, Davide Rossi⁸, Gianluca Gaidano⁸,
Cox Terhorst⁹, Silvia Deaglio^{1,2}

Supplementary Materials and Methods

CLL cell preparation

Peripheral blood mononuclear cells (PBMC) from CLL patients were separated using Ficoll-Hypaque (Sigma) and stained using anti-CD19-FITC and anti-CD5-PE antibodies. If the CD19⁺/CD5⁺ cells were $\geq 95\%$, the sample was used without further treatment. Otherwise PBMC were incubated with a mixture of anti-CD3, anti-CD16 and anti-CD14 antibodies (all at 1 mg/ml) for 30 minutes on ice under continuous agitation. Goat anti-mouse magnetic beads were then added for another 15 minutes before magnetic separation (Life Technologies). Cell purity was checked again by FACS at the end of the procedure.

Antibodies

Anti-SLAMF1 antibodies: anti-SLAMF1-PE (clone A12, eBioscience #12-1509-42, Milan, Italy), -SLAMF1 AlexaFluor647 (clone A12, AbD Serotec # MCA2251A647, Milan, Italy), -SLAMF1 unconjugated, functional grade purified or unconjugated for immunoprecipitation/western blot (clone A12, eBioscience #16-1509-85, Abcam #ab33311 and R&D Systems #MAB1642, respectively). Antibodies for immunofluorescence were: anti-CD19-APC-Vio770 (cat #130-096-643), -CD19-FITC (cat #120-014-229), -CD5-FITC (cat #130-096-574), -CD38-APC (cat #130-092-261) (all from Miltenyi Biotec, Bologna, Italy), -CD49d-PE (cat #130-099-691) and -CD62L-PE-Cy7 (cat #25-0629-42), -CD44 (all from eBioscience), -CXCR3-APC (cat #353708) and CD27 PerCP/Cy5.5 (cat #356408) (both from Biolegend, Rome, Italy). Antibodies against molecules involved in signaling/adhesion or autophagy were: anti-p38 (cat #9212), -p-

p38 (cat #9211), -JNK1/2 (cat #9252), -p-JNK1/2 (cat #94671), -p-BCL2 (Ser70, clone 5H2, cat #2827), -LC3B (cat #2775), -beclin1 (4A10, cat #3495), -PI3 Kinase Class III (D9A5, cat #4263) for immunoprecipitation/western blot (all from Cell Signaling Technology, Rome, Italy), anti-p62 (#610832) and -pan ERK1/2 (cat #610124), both from BD Biosciences, Milan, Italy), -BCL2 (sc-492) and -BCL2-HRP (sc-7382-HRP conjugate) for western blot and -BCL2 (sc-7382) for immunoprecipitation, -LAMP-2 (clone H4B4, sc-18822), -vimentin (V9, cat #sc-6260), -gp91-phox (sc-130543) and -p40-phox (sc-48388), all from Santa Cruz Biotechnology.

The isotype controls used were: anti-mouse Isotype Control FITC/PE/APC/PeCy7/AlexaFluo647 (all from eBioscience).

Secondary antibodies were: DyLight 594-conjugated donkey anti-rabbit IgG (1:100, cat # 711-585-152, Jackson ImmunoResearch, Milan, Italy), AlexaFluor 488-conjugated goat anti-rabbit IgG (1:100, cat #A11008) and goat anti-mouse IgG AlexaFluor 633-conjugated (1:100, cat #A21052) (both from Life Technologies, Milan, Italy), goat anti-mouse IgG-HRP conjugated (cat# NEF822001EA, Perkin Elmer, Milan, Italy), donkey anti-rabbit HRP-conjugated (cat #sc-2313, Santa Cruz Biotechnology), donkey anti-mouse IgG Ab (cat #6410-01, Southern Biotechnology, Milan, Italy).

The anti-actin-HRP-conjugated was from Santa Cruz Biotechnologies. Alexa Fluor 568 Phalloidin was used for actin visualization (1:100) and 4',6-Diamidino-2-phenylindole (DAPI, 1:30000) for nuclear staining (both from Life Technologies).

Irrelevant mAb mouse anti-human X63 was from F. Malavasi (University of Turin, Italy)

Inhibitors

Diphenyleneiodonium (DPI, NOX2 inhibitor) was from Sigma Aldrich (Milan, Italy), SP600125 (JNK1/2 inhibitor) from Selleckchem (Rome, Italy) and N-Acetyl-L-cysteine (NAC) from Santa Cruz Biotechnology.

Primers

All primers were from TaqMan Gene Expression Assays (Life Technologies). They were:

Hs00234149_m1 (*SLAMF1*)

Hs00176908_m1 (*PIK3C3*)

Hs01120071_m1 (*CD38*)

Hs00171041_m1 (*CXCR3*)

Hs00237052_m1 (*CXCR4*)

Hs00185584_m1 (*VIM*)

Hs00174151_m1 (*SELL*)

Hs01075861_m1 (*CD44*)

Hs00984230_m1 (*B2M*)

Hs99999903_m1 (*ACTB*)

Flow cytometry and Cell Sorting

For flow cytometry experiments at least 10,000 events/sample were acquired and analyzed with the Diva8 (BD Biosciences) and FlowJo 9.01 (TreeStar, Ashland, OR, USA) softwares.

For HD CD5⁺ isolation cells were stained using anti-CD19 APC-Vio770, -CD5 FITC and sorted on a FACSaria III (BD Biosciences). To distinguish SLAMF1^{low} and SLAMF1^{high} cells

in CLL clones with bimodal SLAMF1 expression, cells were gated on CD19⁺/CD5⁺ and sorted for the expression of SLAMF1.

Chemotaxis assay

CXCL12/SDF-1 α (100 ng/ml, R&D Systems) and CXCL10 (100 ng/ml, R&D Systems) were used as attractants. The lower chamber of each well contained 600 μ l of RPMI medium supplemented with 0.5% BSA and with chemokines or medium alone. All experiments were carried out in duplicate, measuring chemotaxis in two separate wells for each condition. Samples were counted for 30 seconds under a defined flow rate using a FACSCanto II cytofluorimeter (BD Biosciences) in order to obtain a median of the relative number of total transmigrated cells. The migration was indicated as the number of transmigrated cells in presence of the chemokines for a total input of 10⁵ cells.

Migration of primary CLL cells was performed as previously described (27).

Western blot and immunoprecipitation studies

Cell lysates were resolved by SDS-PAGE and transferred to Mini format 0.2 μ m nitrocellulose membranes (Trans-Blot Turbo Transfer System, Bio-Rad, Segrate, Italy). Blots were incubated with the indicated antibodies and developed by using enhanced chemiluminescence (GE Healthcare). Actin or ERK1/2 confirmed equal protein loading in all conditions. Images were acquired using the LAS4000 imager and bands quantified using the ImageQuant software (GE Healthcare).

For immunoprecipitation studies Mec-1 cells (10⁷) were lysed and immunoprecipitated with Protein G-Sepharose magnetic beads (GE Healthcare) with anti-SLAMF1 (clone A12, Abcam) or irrelevant anti-X63 mAb (0.5 μ g mAb/100 μ g lysate). For immunoprecipitation

experiments with BCL2 (clone C-2, Santa Cruz Biotechnology) or VPS34 (clone D9A5, Cell Signaling Technology) a cross-linking protocol was adopted, according to manufacturer's instructions. Immunoprecipitates were resolved by SDS-PAGE under reducing conditions and analyzed by western blot.

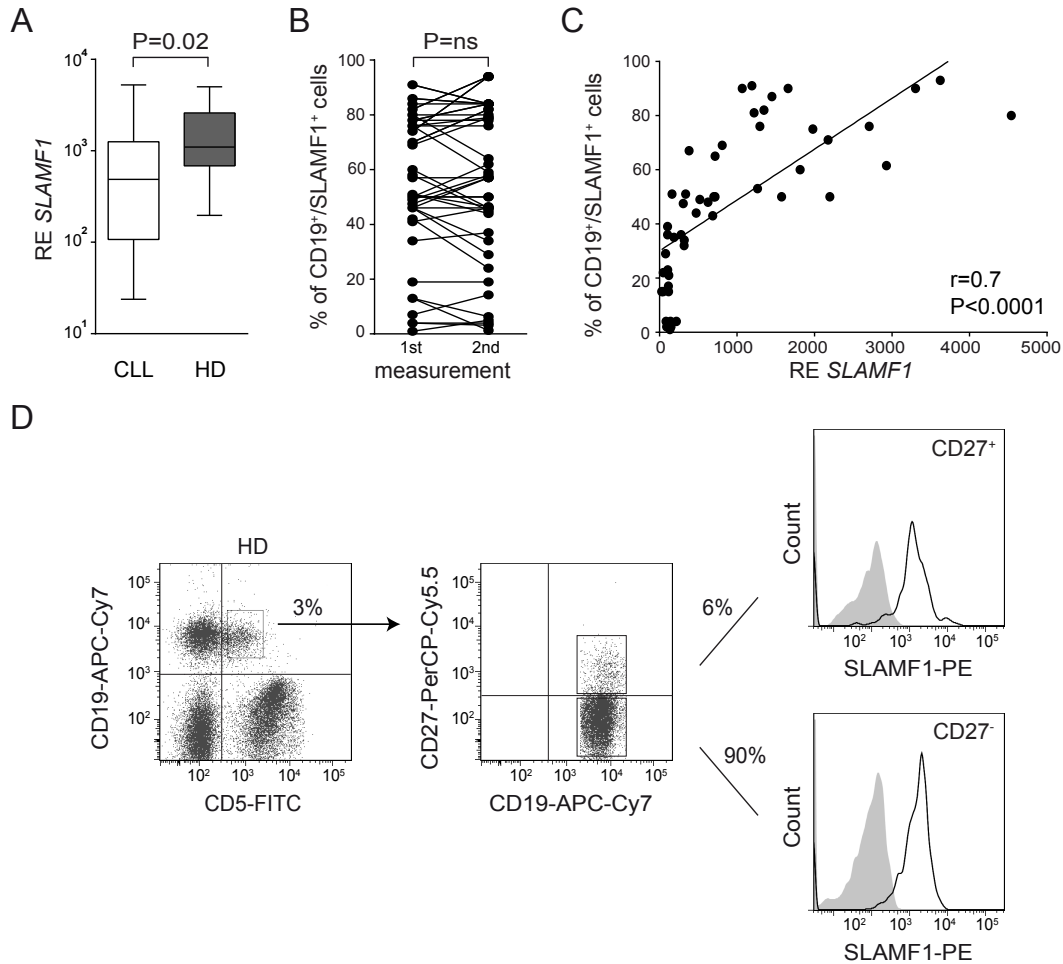
Supplementary Table 1. Main clinical and molecular characteristics of the CLL cohort analyzed in the study.

*: patients were treated with conventional fludarabine- or bendamustine-based regimens, with or without rituximab.

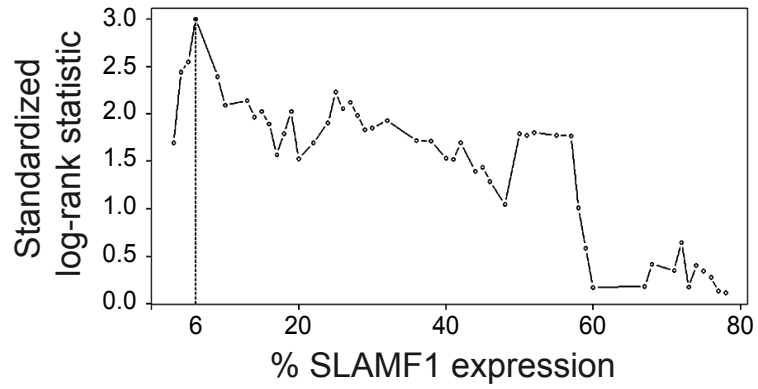
Variable	No. (%)
Patients	300
Median age at diagnosis (years), No.	64
Sex (male)	175 (58.3)
Binet stage at diagnosis	
A	232 (77.3)
B	49 (16.3)
C	17 (5.7)
CD38	
≥30%	115 (38.3)
CD49d, No. 247	
≥30%	100 (40.5)
Treatment*, No. 291	
Treated	129 (44.3)
IgVH gene mutation status, No. 269	
UM (<2%)	100 (37.2)
Genomic aberrations, No. 167	
deletion 11	23 (13.8)
deletion 17	25 (15)
deletion 13	116 (69.5)
trisomy 12	47 (28.1)
normal	101 (60.5)

Supplementary Table 2. List of primers used for mutagenesis and sequencing

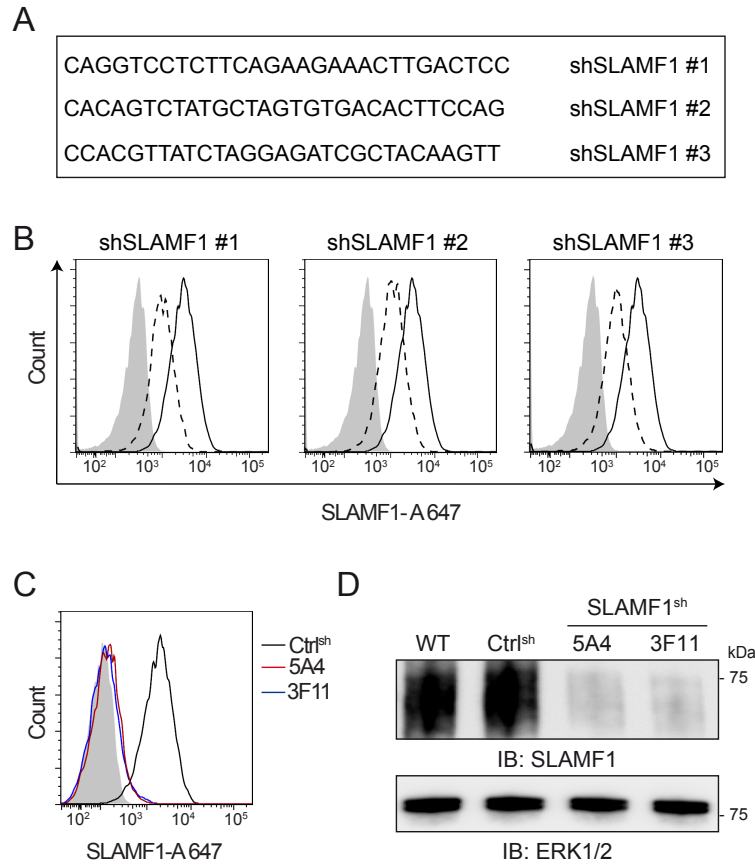
Primer	Sequence
SLAM_mut2F	CCAGAAACCAGGTCCGCTGCAAAGAAACTTGACTCCTTCCC
SLAM_mut2R	GGGAAGGAGTCAAGTTTCTTTGCAGCGGACCTGGTTTCTGG
SLAM_seqF	GGCTGTTAGGGGGTGCATC
SLAM_seqR	TGTTGGTCTCTGGTGCAGC



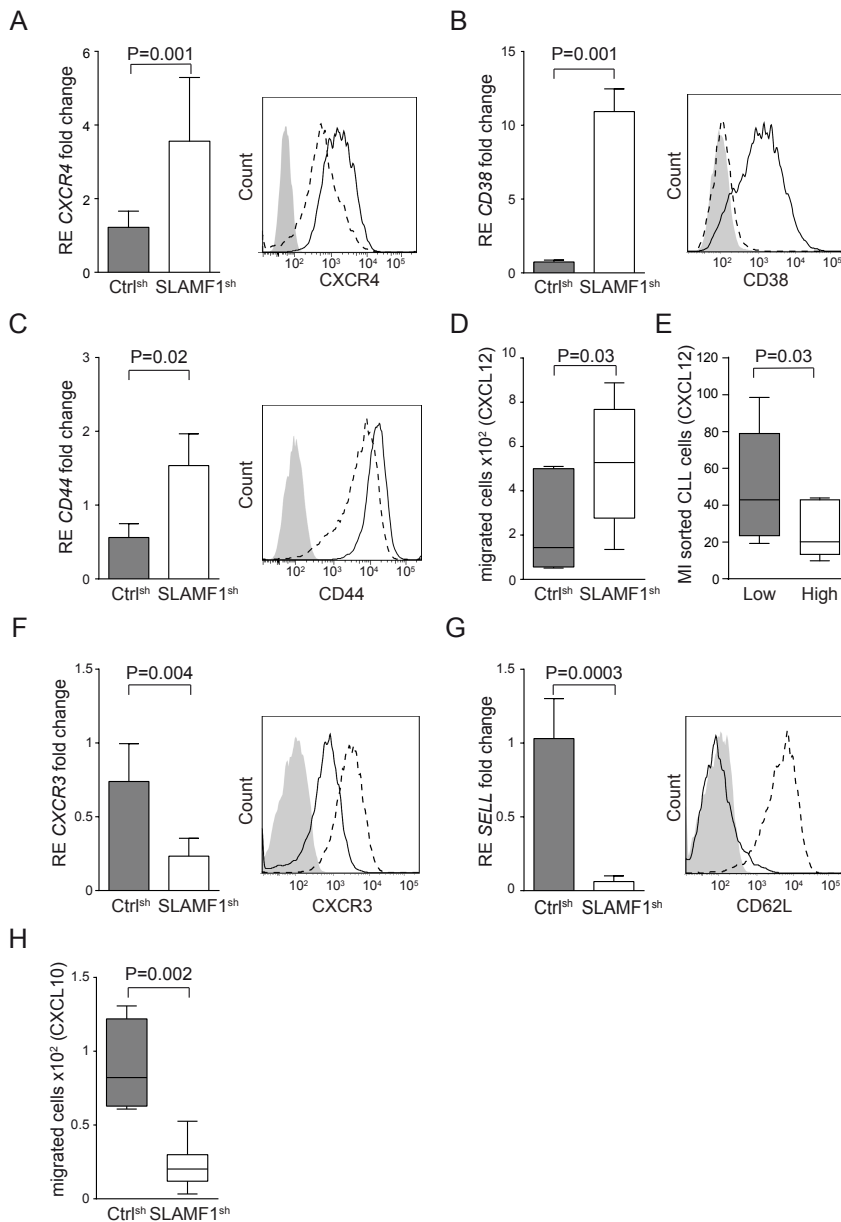
Supplementary Figure 1. SLAMF1 is heterogeneously expressed by CLL cells. (A) qRT-PCR data of SLAMF1 expression relative to ACTB in CD19⁺/CD5⁺ purified CLL cells from 73 CLL patients and from 11 controls. Statistical analysis was performed using Mann-Whitney test. (B) Graph showing the percentage of CD19⁺/SLAMF1⁺ CLL cells in a cohort of 42 patients that were sequentially assessed, at least 3 months apart (range 3-15 months), without intervening therapy. Statistical analysis was performed using Mann-Whitney test. (C) Regression line showing the direct correlation between the percentage of CD19⁺/SLAMF1⁺ cells and the number of SLAMF1 mRNA copies determined by qRT-PCR in 50 patients. Pearson coefficient (r) and the corresponding two-tailed P value are listed. (D) PBMCs from HD were gated on CD5⁺/CD19⁺ and analyzed for SLAMF1 expression in CD27⁺ and CD27⁻ subsets.



Supplementary Figure 2. Definition of an optimal SLAMF1 cut-off value. Recursive partitioning analysis was used to determine the optimal percentage of SLAMF1 expression in the patient cohort analyzed.



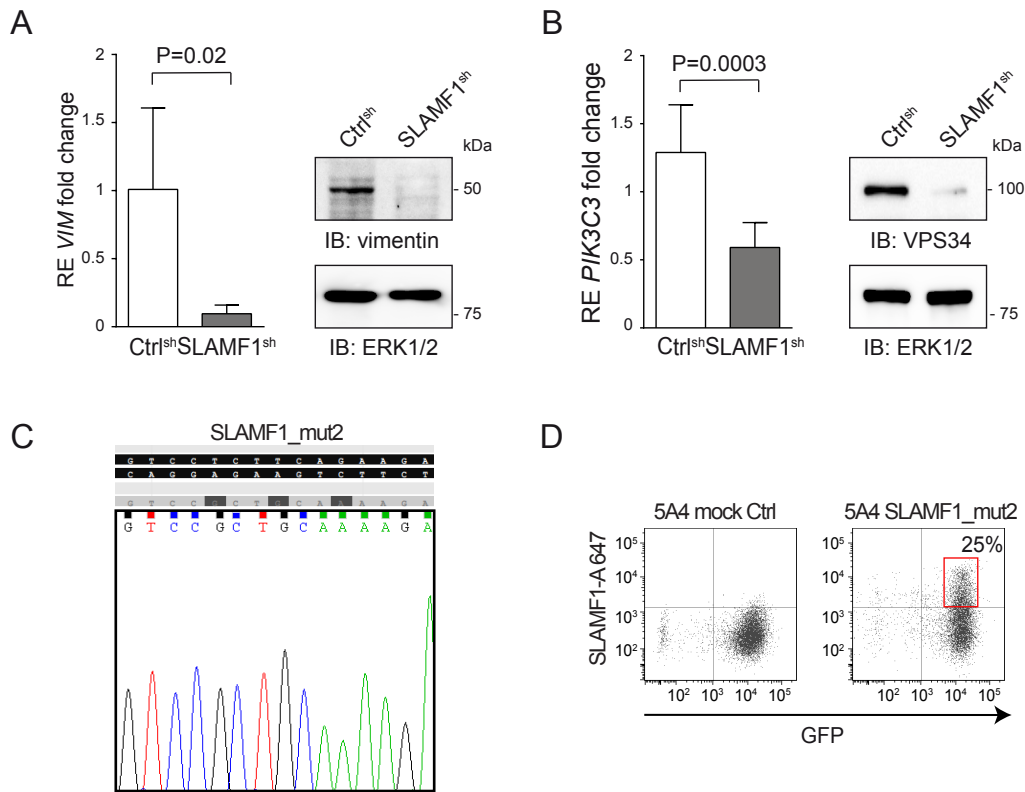
Supplementary Figure 3. Down-modulation of SLAMF1 expression in Mec-1/SLAMF1^{sh} cell clones. (A) Sequences of three SLAMF1 specific shRNAs used for silencing. (B) Immunofluorescence showing SLAMF1 silencing (dashed line) after transient transfection of the three different shRNAs as opposed to a ctrl shRNA (full line). (C) Immunofluorescence and (D) western blot analyses confirm complete silencing of SLAMF1 expression in stably selected Mec-1 clones derived from shRNA#1 (5A4) or from a mixture of the three shRNAs (3F11). **Data in C and D are representative of at least three independent experiments.**



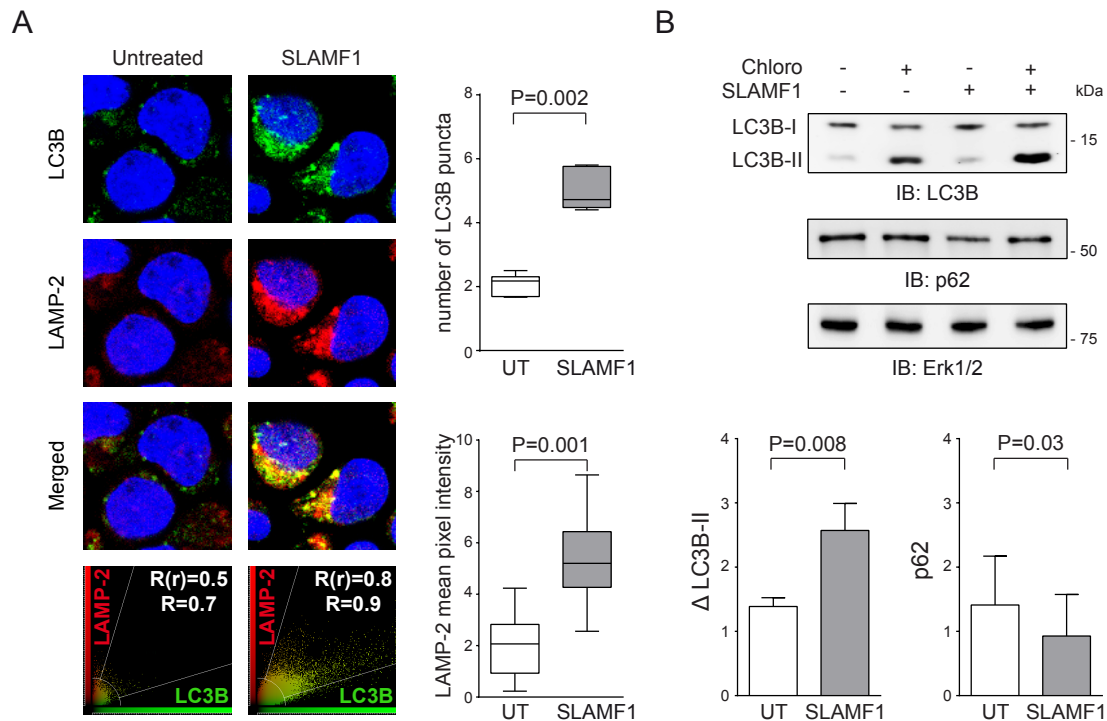
Supplementary Figure 4. Modulation of the expression of genes involved in cell movement and vesicle trafficking in Mec-1/SLAMF1^{sh} cells.

(A-C) qRT-PCR analysis and FACS profiles showing increased expression levels of CXCR4 (A), CD38 (B) and CD44 (C) by Mec-1/SLAMF1^{sh} cells (full line) as opposed to Mec-1/Ctrl^{sh} cells (dotted line). (D) Results from 10 chemotaxis experiments performed with the Mec-1 clones against CXCL12 (100 ng/ml). (E) Results from chemotaxis experiments towards CXCL12 performed by comparing SLAMF^{high} and SLAMF^{low} primary CLL cells sorted from

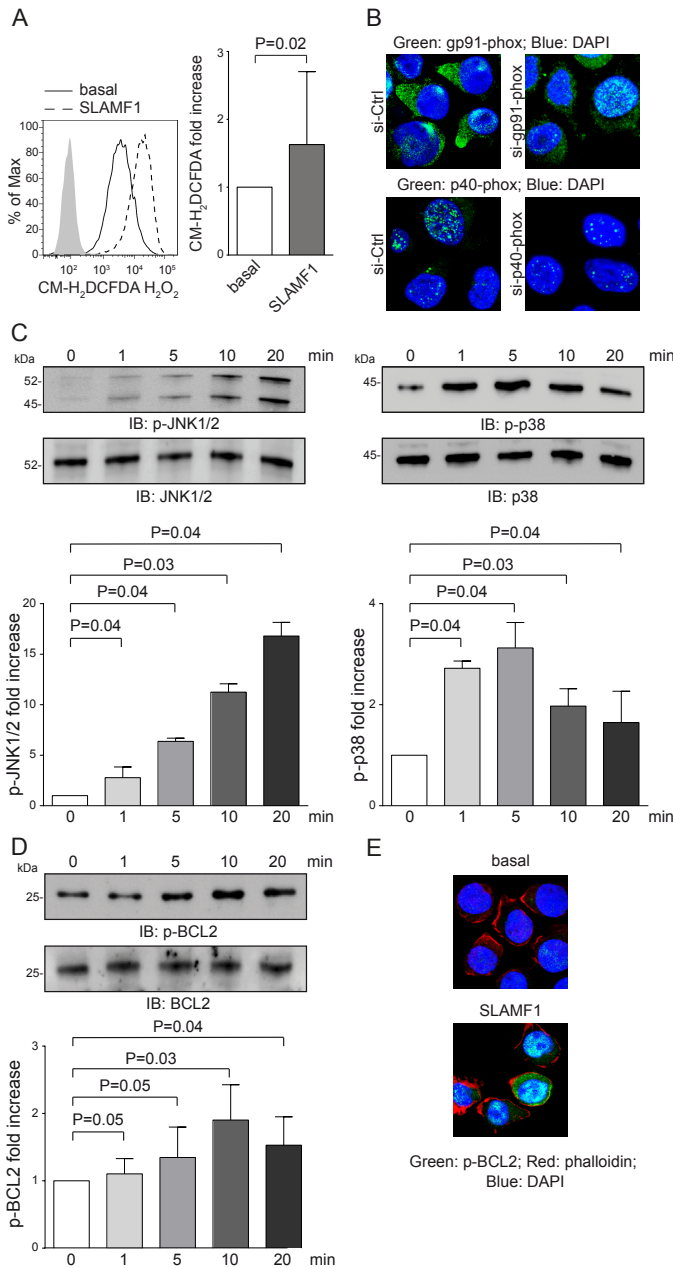
5 independent patients. (F-G) q-RT-PCR analysis and FACS profiles showing decreased expression levels of CXCR3 (F) or SELL/CD62L (G) by Mec-1/SLAMF1^{sh} cells (full line) as opposed to Mec-1/Ctrl^{sh} cells (dotted line). (H) Results from 10 chemotaxis experiments towards CXCL10 performed with the Mec-1 clones. For chemotaxis experiments the number of migrated cells in 600 μ l of medium was measured after 4 hours. The migration index (MI) for primary cells was also determined after 4 hours. The Mann-Whitney test was used to determine statistical significance. qRT-PCR results are expressed relative to the level of Mec-1 wild-type cells, considered to be 1. qRT-PCR data are derived from at least 5 independent experiments for each gene. FACS profiles are representative of at least 5 independent experiments.



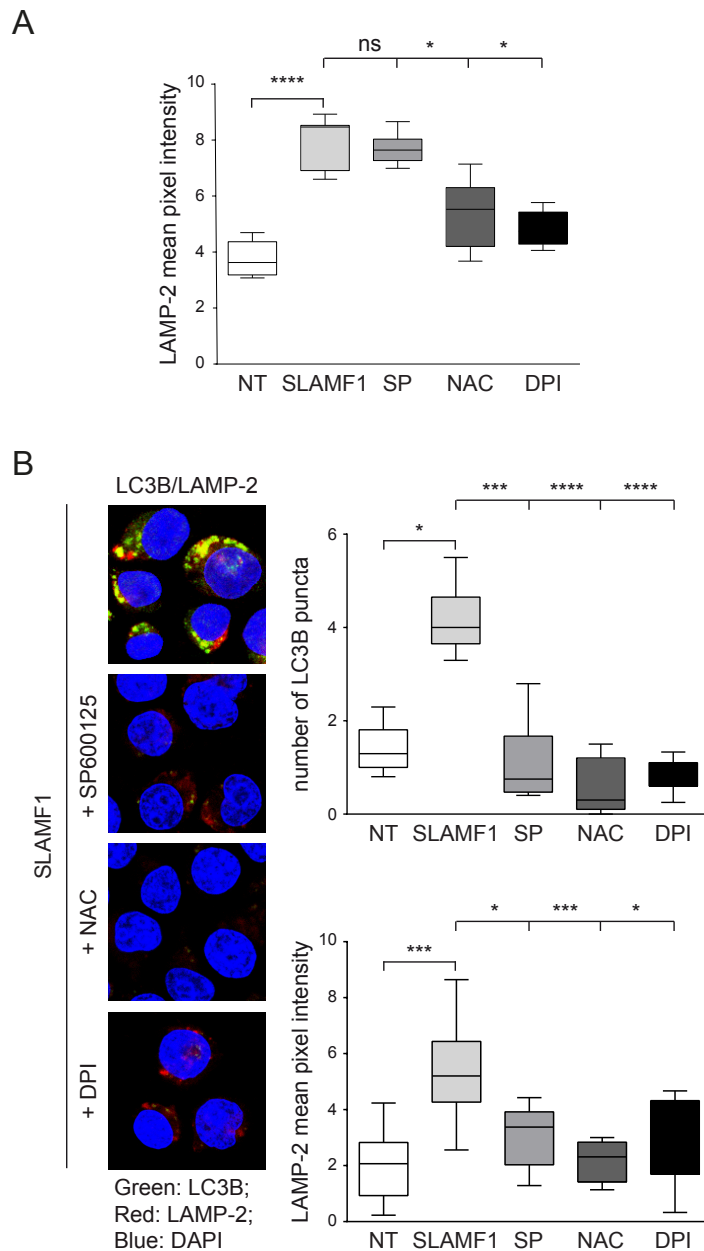
Supplementary Figure 5. Mec-1/SLAMF1^{sh} cells show down-regulation of molecules regulating protein trafficking and autophagy. RT-PCR and western blot analysis showing decreased expression levels of VIM (A) and VPS34 (PIK3C3) (B) in Mec-1/SLAMF1^{sh} cells as opposed to Mec-1/Ctrl^{sh} cells. Statistical analysis was performed using Mann-Whitney test (n=5). (C) Position of synonymous mutations and Sanger sequencing confirmation of mutagenesis performed to generate a SLAMF1 shRNA#1 resistant cDNA clone (SLAMF1_{mut2}). (D) Dot-plots showing reconstitution of SLAMF1 expression after transient transfection of SLAMF1_{mut2} in shRNA#1 derived Mec-1/SLAMF1^{sh} clone 5A4. Red rectangular shows the population FACS-sorted for further RT-PCR analysis. An empty plasmid was used as control (mock).



Supplementary Figure 6. SLAMF1 ligation enhances the autophagic flux in the Mec-1 cell line. (A) Confocal microscopy analysis of LC3B (green) and LAMP-2 (red) staining in Mec-1 cells treated with the agonistic anti-SLAMF1 monoclonal antibody A12, in the presence of coated donkey anti-mouse IgG Ab (24 h, 37 °C). Nuclei were counterstaining with DAPI (blue). Original magnification X63, zoom factor of 2. The box plot shows cumulative numbers of LC3B puncta (calculated as average number of puncta/cell) in cells from 3 **independent** experiments. Quantitative analysis of LAMP-2 mean pixel intensity was performed using ImageJ software (P=0.001). Scatter plots on the bottom represent co-localization analyses between LC3B and LAMP-2 using LAS AF Version Lite 2.4 software (Leica Microsystems). Pearson coefficient (r) and Overlap coefficient (R) are listed. (B) Western blot analysis of LC3B-I/II expression, following SLAMF1 cross-linking in the presence or absence of Chloroquine (Chloro, 15 μ M, 48 h 37°C). Δ LC3B-II levels are an indicator of the autophagic flux and were calculated as the difference of LC3B-II protein levels between Chloroquine-treated and untreated states. Data from 8 independent experiments.



Supplementary Figure 7. Cross-linking of SLAMF1 induces ROS accumulation, activates p38 and JNK1/2 and phosphorylates BCL2. (A) SLAMF1 cross-linking induces ROS accumulation, as measured by flow cytometry using CM-H₂DCFDA dye. Histograms are from a representative experiment. Bar graph shows cumulative data from 6 independent experiments. The Wilcoxon signed-rank test was used to determine statistical significance. (B) Confocal microscopy shows effective silencing of gp91-phox and p40-phox in Mec-1 cells transfected with siRNAs specific for these proteins. Original magnification X63, zoom factor of 2, representative data from 3 independent experiments. (C) Ligation of SLAMF1 on Mec-1 induces time-dependent tyrosine phosphorylation of p38 and JNK1/2. Cumulative data obtained from 4 experiments are shown on the right. The fold increase represents the increase in band intensity over the untreated condition. (D) SLAMF1 cross-linking induces serine phosphorylation of BCL2, peaking after 10 minutes. The graph on the right shows cumulative data from 5 experiments. Statistical analyses for C and D were performed using a two-tailed Student's t test. (E) Confocal microscopy shows that BCL2 is still phosphorylated 6 hours after SLAMF1 cross-linking. Original magnification X63, zoom factor of 2.



Supplementary Figure 8. Use of selective inhibitors to highlight sequential steps in SLAMF1-induced autophagy. (A) Cumulative data of LAMP-2 mean pixel intensity showing the effects of SP600125 (5 μ M), NAC (2.5mM) and DPI (0.05 μ M) on primary CLL cells upon SLAMF1 ligation. Data from 3 different experiments. (B) Confocal microscopy of Mec-1 cells showing the effects of SP600125 (15 μ M), NAC (5mM) and DPI (0.05 μ M) on LC3B induced upon SLAMF1 ligation. Original magnification X63, zoom factor of 2. The box plot shows cumulative numbers of LC3B puncta (calculated as average number of puncta/cell) and mean pixel intensity of LAMP-2 signal from 3 different experiments. Statistical significance was calculated by Friedman's test followed by Dunn's multiple comparison (***) = $p \leq 0.001$, ** = $p \leq 0.01$ and * = $p \leq 0.05$).

References

1. Deaglio, S., Vaisitti, T., Aydin, S., Bergui, L., D'Arena, G., Bonello, L., Omede, P., Scatolini, M., Jaksic, O., Chiorino, G., et al. 2007. CD38 and ZAP-70 are functionally linked and mark CLL cells with high migratory potential. *Blood* 110:4012-4021.